



On the contravariant form of the Navier–Stokes equations in time-dependent curvilinear coordinate systems

Haoxiang Luo ^{*}, Thomas R. Bewley

Flow Control Lab, Dept. of MAE, UC San Diego, La Jolla, CA 92093-0411, USA

Received 30 July 2003; received in revised form 17 November 2003; accepted 14 February 2004
Available online 19 March 2004

Abstract

The contravariant form of the Navier–Stokes equations in a fixed curvilinear coordinate system is well known. However, when the curvilinear coordinate system is time-varying, such as when a body-fitted grid is used to compute the flow over a compliant surface, considerable care is needed to handle the momentum term correctly. The present paper derives the complete contravariant form of the Navier–Stokes equations in a time-dependent curvilinear coordinate system from the intrinsic derivative of contravariant vectors in a moving frame. The result is verified via direct transformation. These complete equations are then applied to compute incompressible flow in a 2D channel with prescribed boundary motion, and the significant effect of some terms which are sometimes either overlooked or assumed to be negligible in such a derivation is quantified.

© 2004 Elsevier Inc. All rights reserved.

Keywords: Contravariant; Navier–Stokes equations; Time-dependent curvilinear coordinates

1. Introduction

The Navier–Stokes equations in a fixed curvilinear coordinate system were established long ago using coordinate transformation; one may find the standard form of these equations and their derivation in tensor calculus textbooks, see [1]. However, such a general form of the Navier–Stokes equations have not been used widely in numerical simulations, since the calculation of the covariant derivatives in curvilinear coordinate systems is generally quite expensive. Many researchers have opted for alternative forms of the Navier–Stokes equations when they deal with flows in complex geometries via mapping into a regular domain. Such an approach can also be applied to time-dependent curvilinear coordinate systems. For example, a formulation is widely used in which Cartesian based velocity components multiplied by the Jacobian of the transformation (i.e., the volume flux components) are used as the flow variables [2,3]. Another commonly used formulation incorporates the velocity vectors in both the Cartesian coordinate

^{*} Corresponding author. Tel.: +1-858-822-3729; fax: +1-858-822-3107.
E-mail address: hxluo@turbulence.ucsd.edu (H. Luo).

system and the curvilinear coordinate system [4–8]. In this formulation, though the contravariant velocity vector is introduced to make the equations simpler, the acceleration of the momentum is ultimately determined in the Cartesian coordinate directions. Voke and Collins [9] proposed a contravariant velocity–vorticity formulation of the Navier–Stokes equations for both compressible and incompressible flows in a fixed general coordinate system. Their formulation avoids explicit use of the connection coefficients and the transformation matrix elements in the governing equations at the expense of the computation of the contravariant form of the vorticity.

Rosenfeld and Kwak [10] presented a discrete contravariant formulation of the incompressible Navier–Stokes equations in generalized moving coordinates using a finite volume method that satisfies the geometric conservation laws for time-varying computational cells. However, the corresponding PDE in the continuous setting is not readily apparent from this inherently discrete formulation.

Under some circumstances, for example, when the transformation is relatively simple, the use of the continuous tensorial formulation of Navier–Stokes equations is manageable. Carlson et al. [11] extended the tensorial formulation to the moving coordinate system case and used direct numerical simulation to calculate turbulence in a channel with time-dependent wall geometries. Their formulation was used later by Xu et al. [12] to simulate turbulent flow over a compliant surface. Because of the specific transformation used in their work, a change in orientation of a vector into the new coordinate system is ascribed only to its wall-normal component and many connection coefficients vanish. However, when deriving the temporal derivative of a vector tensor in a moving frame, one has to be careful, since additional terms may appear due to the moving coordinates. The derivation of Carlson et al. [11] omits some of these potentially important terms. Simply treating the temporal derivative of the contravariant form of the velocity vector in the same way as for a scalar variable, such as density, fails to capture all of the terms in this formulation, thereby possibly compromising the accuracy of the subsequent computations.

Ogawa and Ishiguro [13] also derived the temporal derivative of tensor vectors, as considered in the present work, via a different approach than that used here, specifically, by considering the infinitesimal geometric motion of the curvilinear coordinates. The form of the Navier–Stokes equations they obtained, which is consistent with the present derivation, involves the covariant derivatives of the velocity of the coordinates that are missing in the analysis of Carlson et al. [11]. In the present work, we derive the intrinsic temporal derivative of tensor vectors using an alternative approach, the quotient rule of tensor analysis, and then obtain the complete contravariant form of the Navier–Stokes equations in time-dependent curvilinear coordinate systems. Unlike the derivation of Ogawa and Ishiguro [13], which is based on geometrical arguments, the tensor derivation given in the present paper may be easily generalized to tensorial equations of order higher than one (vectors) if necessary. We also demonstrate use of the equations by applying them to solve flows in 2D channels with moving boundaries. Note that, in addition to approaches based on coordinate transformation, there are many other available techniques for computational fluid dynamics in systems with moving boundaries, e.g., volume tracking methods, level-set methods, and immersed boundary methods, etc. Readers are referred to [14–16] for more information.

2. Derivation of the Navier–Stokes equations in moving coordinate systems

2.1. Equations of motion in a fixed coordinate system

In order to introduce the notation to be used, we first consider a time-invariant transformation $x^i = x^i(\xi^1, \xi^2, \xi^3)$ from the Cartesian coordinates \mathbf{x} to the curvilinear coordinates ξ . (Note that superscripts indicate contravariant components, not powers, in the present notation.) We define the transformation matrix

$$C = \frac{\partial \mathbf{x}}{\partial \boldsymbol{\xi}}, \quad c_j^i = \frac{\partial x^i}{\partial \xi^j}, \tag{1}$$

and its inverse

$$\bar{C} = \frac{\partial \boldsymbol{\xi}}{\partial \mathbf{x}}, \quad \bar{c}_j^i = \frac{\partial \xi^i}{\partial x^j}. \tag{2}$$

The metric tensor and its inverse are defined by

$$g_{ij} = c_i^k c_j^k, \quad g^{ij} = \bar{c}_k^i \bar{c}_k^j, \tag{3}$$

respectively. The Jacobian of the transformation is defined by

$$J = |C|. \tag{4}$$

The transformation relationship between the contravariant velocity vector \mathbf{v} in the Cartesian coordinate system and its counterpart \mathbf{u} in the curvilinear coordinate system is

$$v^j = c_j^i u^i, \quad \text{or} \quad u^i = \bar{c}_j^i v^j. \tag{5}$$

The same relationship also applies to other contravariant vectors.

The mass and momentum conservation equations in contravariant form in a fixed coordinate system may be written as follows [1, pp. 178–179]

$$\begin{aligned} \frac{\partial \rho}{\partial t} + (\rho u^i)_{,i} &= 0, \\ \rho \left(\frac{\partial u^i}{\partial t} + u^j u_{,j}^i \right) &= \rho f^i + T_j^{ij}, \end{aligned} \tag{6}$$

where the contravariant vector f^i is the external body force per unit mass and T^{ij} is the contravariant stress tensor. In the above equations, a comma with an index in a subscript denotes covariant differentiation:

$$u_{,j}^i = \frac{\partial u^i}{\partial \xi^j} + \Gamma_{jk}^i u^k, \tag{7}$$

where Γ_{jk}^i are the components of connection coefficients, also known as the Christoffel symbol of the second kind. Now consider a time-dependent transformation from a Cartesian coordinate system \mathbf{x} to a curvilinear coordinate system $\boldsymbol{\xi}$

$$\begin{cases} x^i = x^i(\xi^1, \xi^2, \xi^3, \tau), \\ t = \tau. \end{cases} \tag{8}$$

It is tempting (see, e.g., the derivations of Carlson et al. [11]) to simply apply the chain rule

$$\frac{\partial}{\partial t} \rightarrow \frac{\partial}{\partial \tau} + \frac{\partial \xi^j}{\partial t} \frac{\partial}{\partial \xi^j} \tag{9}$$

and the relations (1)–(5) in order to re-express the temporal derivative terms in (6) and to cast it in the moving coordinate system. But is this correct? The answer is not obvious for an equation as complicated as (6). However, we may use a simple counterexample to show that such a simple substitution in fact misses some terms which are sometimes important. Consider a uniform flow free from the external force. Its velocity components in the Cartesian coordinate system are $v^1 = 1, v^2 = v^3 = 0$. Suppose we use the following coordinate transformation:

$$\begin{cases} x^1 = \xi^1 \cos \tau - \xi^2 \sin \tau, \\ x^2 = \xi^1 \sin \tau + \xi^2 \cos \tau, \end{cases} \quad C = \begin{pmatrix} \cos \tau & -\sin \tau \\ \sin \tau & \cos \tau \end{pmatrix}, \quad \bar{C} = \begin{pmatrix} \cos \tau & \sin \tau \\ -\sin \tau & \cos \tau \end{pmatrix}, \quad (10)$$

which simply means that the new coordinate system is rotating counterclockwise at a constant speed. We can see immediately [by (5)] that the velocity components in the new coordinate system are $u^1 = \cos \tau$, $u^2 = -\sin \tau$ (the third component is neglected since this is a two-dimensional problem). Since \mathbf{u} is independent of ξ , and the connection coefficients Γ_{jk}^i are all zero, by (7) we have $u^i_{,j} = 0$. However, applying (9) would produce the momentum equation

$$\frac{\partial u^i}{\partial t} = \frac{\partial u^i}{\partial \tau} + \frac{\partial \xi^j}{\partial t} \frac{\partial u^i}{\partial \xi^j} = \frac{\partial u^i}{\partial \tau} = 0, \quad (11)$$

which is clearly incorrect. Apparently, the Coriolis force is not correctly accounted for in the rotating coordinates by following this approach.

To solve the apparent dilemma, we examine the intrinsic temporal derivative of a tensor vector in a moving frame and apply the differentiation to the contravariant velocity vector while using Reynolds' transport theorem to derive correctly the desired form of the Navier–Stokes equations.

We shall rewrite the definition of Γ_{jk}^i , the Christoffel symbol of the second kind, to facilitate this derivation. The common definition of the Christoffel symbol is given by

$$\Gamma_{jk}^i = g^{ip}[jk, p] = \frac{1}{2}g^{ip} \left(\frac{\partial g_{pj}}{\partial \xi^k} + \frac{\partial g_{pk}}{\partial \xi^j} - \frac{\partial g_{jk}}{\partial \xi^p} \right),$$

where $[jk, p]$ is the Christoffel symbol of the first kind, as defined in [1, p. 162] by

$$[jk, p] = \frac{1}{2} \left(\frac{\partial g_{pj}}{\partial \xi^k} + \frac{\partial g_{pk}}{\partial \xi^j} - \frac{\partial g_{jk}}{\partial \xi^p} \right) = \sum_m \left[\frac{\partial x^m}{\partial \xi^p} \frac{\partial}{\partial \xi^j} \left(\frac{\partial x^m}{\partial \xi^k} \right) \right] = c_p^m \frac{\partial c_k^m}{\partial \xi^j}.$$

The Christoffel symbol of the second kind may thus be written

$$\Gamma_{jk}^i = g^{ip}[jk, p] = \bar{c}_i^p \bar{c}_l^p c_p^m \frac{\partial c_k^m}{\partial \xi^j} = \bar{c}_l^i \delta_l^m \frac{\partial c_k^m}{\partial \xi^j} = \bar{c}_l^i \frac{\partial c_k^l}{\partial \xi^j}. \quad (12)$$

2.2. The intrinsic derivative

We now follow the procedure in [1, p. 166] to derive the intrinsic derivative. Consider a time-dependent coordinate transformation (8). The velocity vectors of the moving coordinates are

$$\bar{U}^i = \frac{\partial x^i}{\partial \tau}, \quad \text{and} \quad U^j = -\frac{\partial \xi^j}{\partial t} \quad (13)$$

in the Cartesian space and curvilinear space, respectively, and they satisfy the contravariant transformation rule, i.e., $\bar{U}^i = c^i_j U^j$.

Let \bar{B}_i be an arbitrary parallel covariant vector field with constant components in Cartesian space (\mathbf{x}, t) , and B_i be its covariant counterpart in the curvilinear space (ξ, τ) . Consider a curve describing the path of a fluid particle, parameterized by $x^i(t)$ and $\xi^i(t)$ in the two coordinate systems, respectively. Note that $\xi^i(t)$ can be determined from $x^i(t)$ and the implicit function $\xi^i = \xi^i(x^j, t)$ implied by the transformation (8). The two parametric equations $\mathbf{x}(t)$ and $\xi(t)$ satisfy

$$\frac{d\xi^k}{dt} = \frac{\partial \xi^k}{\partial t} + \frac{\partial \xi^k}{\partial x^p} \frac{dx^p}{dt} = -U^k + \bar{c}_p^k v^p = -U^k + u^k, \quad (14)$$

where $v^p = \frac{dx^p}{dt}$ and $u^k = \bar{c}_p^k v^p$ are the velocities of the particle in the Cartesian space and curvilinear space, respectively. We are now looking for a derivative with respect to t , namely the intrinsic derivative, denoted as $\frac{D}{Dt}$, which meets two requirements: (1) it should reflect the total variation of a tensor vector along the curve due to infinitesimal change of t (correspondingly, in Cartesian coordinates, this derivative will reduce to the material derivative), and (2) it should preserve tensor character so that it can be applied to any coordinate system. By the first requirement, $\frac{DB_i}{Dt}$ should vanish along the curve, as B_i represents physically the same constant parallel vector field as \bar{B}_i . Since we have $\frac{D\bar{B}_i}{Dt} = \frac{dB_i}{Dt} = 0$, which holds for all points along the curve, this condition is

$$\frac{d\bar{B}_i}{dt} = \frac{d}{dt}(\bar{c}_i^j B_j) = \bar{c}_i^j \frac{dB_j}{dt} + B_j \frac{d\bar{c}_i^j}{dt} = 0. \tag{15}$$

Multiplying this equation by c_r^i and summing over i , noting that $c_r^i \bar{c}_i^j = \delta_r^j$, we obtain the condition for the covariant B_r to be a parallel field,

$$\frac{dB_r}{dt} + B_j c_r^i \frac{d\bar{c}_i^j}{dt} = 0. \tag{16}$$

This suggests that, for a covariant vector B_r , the intrinsic derivative we are seeking is

$$\frac{DB_r}{Dt} = \frac{dB_r}{dt} + B_j c_r^i \frac{d\bar{c}_i^j}{dt},$$

which indeed satisfies both requirements [fulfillment of the second requirement is seen from the derivation of (16), noting that $\frac{DB_r}{Dt} = c_r^i \frac{D\bar{B}_i}{Dt}$]. In the same way, we may obtain a similar derivative for a parallel contravariant vector field.

More generally, we now use the quotient rule to derive the tensor character for such a derivative of an arbitrary contravariant vector field. Switching dummy indices in (16) by $i \rightarrow l$, and then $r \rightarrow i$,

$$\frac{dB_i}{dt} = -B_j c_i^l \frac{d\bar{c}_l^j}{dt} = B_j \left(\bar{c}_l^j \frac{dc_i^l}{dt} - \frac{dc_l^j \bar{c}_l^j}{dt} \right) = B_j \left(\bar{c}_l^j \frac{dc_i^l}{dt} - \frac{d\delta_l^j}{dt} \right) = B_j \bar{c}_l^j \frac{dc_i^l}{dt}. \tag{17}$$

Now let A^i be any time-varying contravariant vector field in (ξ, τ) -space. Then $A^i B_i$ and its derivative along the curve $\xi(t)$, $\frac{d(A^i B_i)}{dt}$, are both scalars which are independent of the coordinate systems. However, by (17)

$$\frac{d(A^i B_i)}{dt} = \frac{dA^i}{dt} B_i + A^i \frac{dB_i}{dt} = \frac{dA^i}{dt} B_i + A^i B_j \bar{c}_l^j \frac{dc_i^l}{dt} = \left(\frac{dA^i}{dt} + A^i \bar{c}_l^j \frac{dc_i^l}{dt} \right) B_j. \tag{18}$$

Note that the dummy index i in the first term has been switched to j . Since $\frac{d(A^i B_i)}{dt}$ is a scalar tensor and B_j is an arbitrary covariant vector, the quotient rule implies that the term in brackets is a contravariant vector. It is the intrinsic derivative we are seeking and may be written as

$$\frac{DA^j}{Dt} = \frac{dA^j}{dt} + A^i \bar{c}_l^j \frac{dc_i^l}{dt}. \tag{19}$$

Note that the material derivative $\frac{d}{dt}$ along the curve $\xi(t)$ is

$$\frac{d}{dt} = \frac{\partial}{\partial \tau} \frac{d\tau}{dt} + \frac{\partial}{\partial \xi^k} \frac{d\xi^k}{dt} = \frac{\partial}{\partial \tau} + \frac{\partial}{\partial \xi^k} \frac{d\xi^k}{dt}. \tag{20}$$

Substitute (14) and (20) into (19), and the intrinsic derivative becomes

$$\begin{aligned} \frac{DA^j}{Dt} &= \frac{\partial A^j}{\partial \tau} + \frac{\partial A^j}{\partial \xi^k} \frac{d\xi^k}{dt} + A^i \bar{c}_l^j \left(\frac{\partial c_l^i}{\partial \tau} + \frac{\partial c_l^i}{\partial \xi^k} \frac{d\xi^k}{dt} \right) = \frac{\partial A^j}{\partial \tau} + \left(\frac{\partial A^j}{\partial \xi^k} + A^i \bar{c}_l^j \frac{\partial c_l^i}{\partial \xi^k} \right) \frac{d\xi^k}{dt} + A^i \bar{c}_l^j \frac{\partial c_l^i}{\partial \tau} \\ &= \frac{\partial A^j}{\partial \tau} + \left(\frac{\partial A^j}{\partial \xi^k} + \Gamma_{ki}^j A^i \right) \frac{d\xi^k}{dt} + A^i \bar{c}_l^j \frac{\partial c_l^i}{\partial \tau} = \frac{\partial A^j}{\partial \tau} + A^i_{,k} (u^k - U^k) + A^i \bar{c}_l^j \frac{\partial c_l^i}{\partial \tau}, \end{aligned} \quad (21)$$

where the definition of Christoffel symbol of the second kind in (12) has been used. Furthermore, since

$$\frac{\partial c_l^i}{\partial \tau} = \frac{\partial}{\partial \tau} \left(\frac{\partial x^l}{\partial \xi^i} \right) = \frac{\partial}{\partial \xi^i} \left(\frac{\partial x^l}{\partial \tau} \right) = \frac{\partial \bar{U}^l}{\partial \xi^i} = \frac{\partial x^k}{\partial \xi^i} \frac{\partial \bar{U}^l}{\partial x^k} = \frac{\partial x^k}{\partial \xi^i} \bar{U}^l_{,k},$$

where the covariant derivative and partial derivative are the same in Cartesian space, and $\bar{U}^l_{,k}$ is actually a mixed second order tensor, then

$$\bar{c}_l^j \frac{\partial c_l^i}{\partial \tau} = \bar{c}_l^j c_i^k \bar{U}^l_{,k} = U^j_{,i}. \quad (22)$$

Finally, the intrinsic derivative of the contravariant vector A^j becomes

$$\frac{DA^j}{Dt} = \frac{\partial A^j}{\partial \tau} + A^i_{,i} (u^i - U^i) + A^i U^j_{,i}. \quad (23)$$

The additional terms that arise in the intrinsic temporal differentiation are due to the motion of the base vectors which are also spatially varying. To see this let us consider a Cartesian vector

$$\bar{\mathbf{a}} = a^j \mathbf{e}_{(j)},$$

where the coefficient a^j is the component of the contravariant counterpart of $\bar{\mathbf{a}}$ in the curvilinear coordinate system (ξ, τ) , and $\mathbf{e}_{(j)}$ is a set of Cartesian base vectors for (ξ, τ) -coordinates, defined by $e_{(j)}^i = \frac{\partial x^i}{\partial \xi^j} = c_j^i$. The derivative of $\bar{\mathbf{a}}$ with respect to t along the curve $\xi(t)$ is

$$\frac{d\bar{\mathbf{a}}}{dt} = \frac{\partial \bar{\mathbf{a}}}{\partial \tau} + \frac{\partial \bar{\mathbf{a}}}{\partial \xi^i} \frac{d\xi^i}{dt} = \frac{\partial a^j}{\partial \tau} \mathbf{e}_{(j)} + a^j \frac{\partial \mathbf{e}_{(j)}}{\partial \tau} + \left(\frac{\partial a^j}{\partial \xi^i} \mathbf{e}_{(j)} + a^j \frac{\partial \mathbf{e}_{(j)}}{\partial \xi^i} \right) \frac{d\xi^i}{dt} = \left[\frac{\partial a^j}{\partial \tau} + a^i U^j_{,i} + a^j_{,i} \frac{d\xi^i}{dt} \right] \mathbf{e}_{(j)}, \quad (24)$$

where the definition of $\mathbf{e}_{(j)}$, Eqs. (12) and (22) have been used to show $\frac{\partial \mathbf{e}_{(j)}}{\partial \tau} = U^i_{,j} \mathbf{e}_{(i)}$ and $\frac{\partial \mathbf{e}_{(j)}}{\partial \xi^i} = \Gamma_{ji}^k \mathbf{e}_{(k)}$, and the dummy indices are swapped to complete the derivation. The expression in brackets is just the contravariant form of the intrinsic derivative and shows that the additional terms come in with both the temporal and spatial variability of the base vectors.

It should be pointed out this differentiation is not the same as the convective derivative, as described in [17] and [1, p. 185], which is used to study inherent material properties, especially for non-Newtonian flows, even if our moving coordinates are chosen to be the material coordinates in which case the intrinsic derivative reduces to $\frac{DA^j}{Dt} = \frac{\partial A^j}{\partial \tau} + A^i U^j_{,i}$. The convective derivative is simply $\frac{\partial A^j}{\partial \tau}$, which reflects the rate of change of A^j in material coordinates. Note that the convective derivative $\frac{\partial A^j}{\partial \tau}$, when expressed in the fixed curvilinear coordinates, has an involved form reminiscent of (23), but represents something different. The intrinsic derivative $\frac{DA^j}{Dt}$ also takes into account the change caused by the motion of material coordinates themselves.

2.3. Equations of motion in a moving coordinate system

We now apply Reynolds' transport theorem. Let $F(\xi, \tau)$ be any function and $V(t)$ be a closed volume moving with the fluid. Then

$$\frac{D}{Dt} \int \int \int_{V(t)} F dV = \int \int \int_{V(t)} \left[\frac{DF}{Dt} + Fu^i_{,i} \right] dV \quad (25)$$

holds for any tensor F . If F is a scalar, e.g., $F = \rho$, then the term $A^i U_j^j$ in (23) does not exist and the covariant derivative reduces to the partial derivative, so we have $\frac{D\rho}{Dt} = \frac{\partial\rho}{\partial t} + \frac{\partial\rho}{\partial \xi^i} (u^i - U^i)$. By the mass conservation law we require the integration in (25) to vanish, and thus obtain the continuity equation

$$\frac{\partial\rho}{\partial\tau} - \frac{\partial\rho}{\partial\xi^i} U^i + (\rho u^i)_{,i} = 0, \tag{26}$$

which, incidentally, is exactly the same as what we get by replacing (9) into the mass conservation equation in (6) in a fixed curvilinear coordinate system. The temporal terms in the energy conservation equation transform in a similar manner.

If $F = \rho u^i$ is the momentum vector, by the definition of the intrinsic derivative in (23) and the momentum conservation law, we have

$$\begin{aligned} \frac{D}{Dt} \int \int \int_{V(t)} \rho u^i dV &= \int \int \int_{V(t)} \left[\frac{\partial\rho u^i}{\partial\tau} + (u^j - U^j)(\rho u^i)_{,j} + \rho u^j U_{,j}^i + \rho u^i u_{,j}^j \right] dV \\ &= \int \int \int_{V(t)} [\rho f^i + T_j^{ij}] dV. \end{aligned} \tag{27}$$

Therefore the momentum conservation equation may be written

$$\frac{\partial u^i}{\partial\tau} + (u^j - U^j)u_{,j}^i + u^j U_{,j}^i = f^i + \frac{1}{\rho} T_j^{ij}. \tag{28}$$

Note that the continuity Eq. (26) has been substituted to make the above equation simpler.

When the ξ coordinate system is fixed, i.e., $U^j = 0$, then the Eqs. (26) and (28) reduce to (6) as expected. Conversely, however, the extra terms which arise from the temporal intrinsic differentiation of a tensor vector, $-U^j u_{,j}^i + u^j U_{,j}^i$, are not obviously seen in (6). Simply applying the chain rule (9) for temporal differentiation in the momentum conservation equation in (6) instead produces $-U^j \frac{\partial u^i}{\partial \xi^j}$, which is not equivalent to $-U^j u_{,j}^i + u^j U_{,j}^i$.

2.4. Example: uniform flow in a rotating coordinate system

We now re-examine the example of the uniform flow in a spinning coordinate system, as introduced in (10). The velocity of the spinning coordinate system is

$$\mathbf{U} = -\frac{\partial \boldsymbol{\xi}}{\partial t} = \begin{pmatrix} \sin t & -\cos t \\ \cos t & \sin t \end{pmatrix} \begin{pmatrix} x^1 \\ x^2 \end{pmatrix} = \begin{pmatrix} -\xi^2 \\ \xi^1 \end{pmatrix}.$$

Since the covariant differentiation reduces to partial differentiation in this case and $u_j^i = 0$, in this example Eq. (28) reduces to

$$\frac{\partial u^i}{\partial\tau} + u^j U_{,j}^i = 0,$$

which may be written

$$\begin{pmatrix} -\sin \tau \\ -\cos \tau \end{pmatrix} + \begin{pmatrix} 0 & -1 \\ 1 & 0 \end{pmatrix} \begin{pmatrix} \cos \tau \\ -\sin \tau \end{pmatrix} = \mathbf{0}.$$

Thus, (28) is seen to hold in the present example.

2.5. Example: stagnation point flow in a material coordinate system

When $U^j = u^j$, that is, the velocity of the coordinate coincides with the velocity of the fluid, as Ogawa and Ishiguro [13] pointed out, Eqs. (26) and (28) become the expressions in Lagrange coordinates, or material coordinates, which are often used to describe the mechanics of solids. We now consider the problem of stagnation point flow where the Cartesian velocity components and pressure (divided by the constant density) are given by, $v^1 = \alpha x^1$, $v^2 = -\alpha x^2$, $p = -\frac{\alpha^2}{2}[(x^1)^2 + (x^2)^2]$, and α is a constant scalar. The velocity vector satisfies the Cartesian momentum equation which, in terms of the material derivative, reduces to

$$\frac{dv^i}{dt} = \bar{d}^i = \begin{pmatrix} \alpha^2 x^1 \\ \alpha^2 x^2 \end{pmatrix}, \quad (29)$$

where \bar{d}^i is the contravariant pressure gradient vector divided by the density in Cartesian space. Motivated by (29), we define the material coordinate system

$$\begin{cases} \xi^1 = x^1 e^{-\alpha t} \\ \xi^2 = x^2 e^{\alpha t} \end{cases}, \quad C = \begin{pmatrix} e^{\alpha t} & 0 \\ 0 & e^{-\alpha t} \end{pmatrix}, \quad \bar{C} = \begin{pmatrix} e^{-\alpha t} & 0 \\ 0 & e^{\alpha t} \end{pmatrix}.$$

Note that in this special flow, the lines $\xi^1 = \text{constant}$ remain parallel to the x^2 axis and the lines $\xi^2 = \text{constant}$ remain parallel to the x^1 axis though these lines move along with the fluid particles. Since $U^j = u^j$, the contravariant form of the momentum conservation Eq. (28) in this example reduces to

$$\frac{\partial u^i}{\partial \tau} + u^j U_j^i = d^i, \quad (30)$$

where d^i denotes the counterpart of \bar{d}^i in the new coordinate system. Note that, by the definition of \mathbf{u} , we have

$$\mathbf{u} = \mathbf{U} = -\frac{\partial \boldsymbol{\xi}}{\partial t} = \begin{pmatrix} \alpha \xi^1 \\ -\alpha \xi^2 \end{pmatrix},$$

and by the relationship between contravariant vectors we have

$$\mathbf{d} = \bar{C} \bar{\mathbf{d}} = \begin{pmatrix} \alpha^2 \xi^1 \\ \alpha^2 \xi^2 \end{pmatrix},$$

so that, again, (28) is seen to hold in the present example.

As it can be seen, in both examples, although the coordinate systems are orthogonal, the extra terms arising from temporal differentiation of tensor vectors in a moving frame do not vanish.

3. Derivation by direct transformation

The Navier–Stokes equations in a time-dependent curvilinear coordinate system may also be obtained by directly transforming the equations in Cartesian system using the chain rule, though this approach is somewhat cumbersome and does not shed any additional light on the derivation or its physical significance. That is, taking the Cartesian-based momentum equation

$$\frac{\partial v^i}{\partial t} + v^k \frac{\partial v^i}{\partial x^k} = \bar{f}^i + \frac{1}{\rho} \frac{\partial \bar{T}^{ik}}{\partial x^k}, \quad (31)$$

where \bar{f}^i and \bar{T}^{ik} are the counterparts of f^i and T^{ik} respectively in Cartesian space, we may transform the equation by applying chain rule to all the derivatives, substituting \mathbf{v} with \mathbf{u} , multiplying it by \bar{c}_i^j and invoking index summation. From a physical perspective, this means projecting the momentum equation into the new coordinate system. We show here how the transformation of the temporal term is handled, which is the term of interest in this paper.

$$\begin{aligned} \bar{c}_i^j \frac{\partial v^j}{\partial t} &= \bar{c}_i^j \left[\frac{\partial c_k^i u^k}{\partial \tau} + \frac{\partial \xi^l}{\partial t} \frac{\partial c_k^i u^k}{\partial \xi^l} \right] = \frac{\partial u^j}{\partial \tau} + \bar{c}_i^j \frac{\partial c_k^i}{\partial \tau} u^k + \frac{\partial \xi^l}{\partial t} \left(\bar{c}_i^j c_k^i \frac{\partial u^k}{\partial \xi^l} + \bar{c}_i^j \frac{\partial c_k^i}{\partial \xi^l} u^k \right) \\ &= \frac{\partial u^j}{\partial \tau} + u^k U_{,k}^j - U^l \left(\frac{\partial u^j}{\partial \xi^l} + \Gamma_{lk}^j u^k \right) = \frac{\partial u^j}{\partial \tau} + u^i U_{,i}^j - U^i u_{,i}^j. \end{aligned} \tag{32}$$

Similarly, the inertial term becomes

$$\bar{c}_i^j v^k \frac{\partial v^j}{\partial x^k} = u^i u_{,i}^j. \tag{33}$$

Clearly, (32) and (33) add up to the left-hand side of (28).

4. Application: flow in a channel with moving walls

A practical example of the use of such coordinate transformation is to compute the flow in a channel with moving walls. Consider first an incompressible flow in a periodic channel of length L_x whose two walls slightly deform about their nominal locations ($x^2 = 1$ and $x^2 = -1$) continuously with respect to time, as depicted in Fig. 1. In the present study it is sufficient to demonstrate the relevant points in two dimensions; extension to three dimensions, though involved, is straightforward.

If we define $\eta_u(\xi^1, \tau)$ and $\eta_l(\xi^1, \tau)$ to be upper and lower wall displacement from their nominal positions, respectively, in the wall normal direction, and $\eta_1 = (\eta_u - \eta_l)/2$, $\eta_0 = (\eta_u + \eta_l)/2$, then the time-dependent transformation

$$\begin{cases} x^1 = \xi^1, \\ x^2 = \xi^2(1 + \eta_1) + \eta_0, \\ t = \tau \end{cases} \tag{34}$$

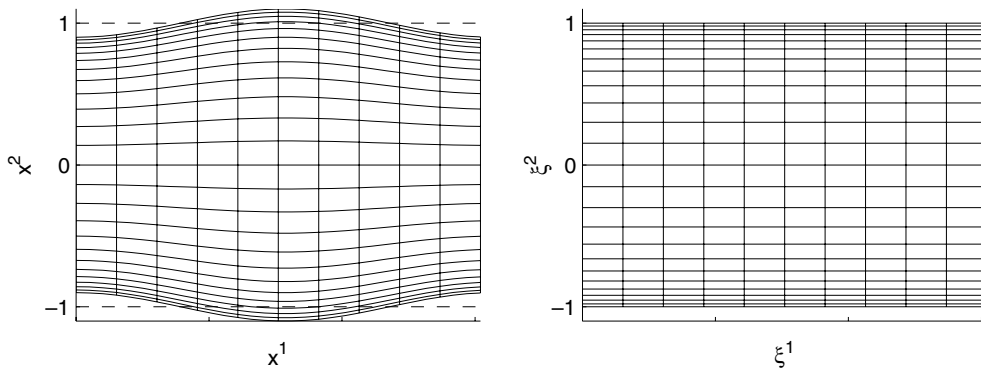


Fig. 1. Physical domain and the computational domain.

may be applied to transform the deformed domain into a rectangular domain. The time-independent version of this transformation has been used by Gal-Chen and Somerville [18,19] to simulate the meteorological phenomena of up-slope winds above a mountainous terrain. Carlson et al. [11] and Kang and Choi [20] used the three-dimensional version of the transformation to calculate turbulence in compliant channels. Note that conformal mapping or orthogonal transformation could be used to solve the present two-dimensional test problem with significantly less effort. However, our main purpose here is to illustrate a particular issue in general coordinate transformation on a 2D test problem.

By definitions (1)–(4), we have (2×2 instead of 3×3 matrices are considered for this 2D problem)

$$C = \begin{pmatrix} 1 & 0 \\ \frac{\partial x^2}{\partial \xi^1} & \frac{\partial x^2}{\partial \xi^2} \end{pmatrix}, \quad \bar{C} = \begin{pmatrix} 1 & 0 \\ -\frac{1}{J} \frac{\partial x^2}{\partial \xi^1} & \frac{1}{J} \end{pmatrix},$$

$$J = |C| = \frac{\partial x^2}{\partial \xi^2} = 1 + \eta_1, \quad \frac{\partial \xi^i}{\partial t} = \begin{pmatrix} 0 \\ -\frac{1}{J} \frac{\partial x^2}{\partial \tau} \end{pmatrix},$$

and the connection coefficients are

$$\Gamma_{jk}^1 = \Gamma_{22}^2 = 0,$$

$$\Gamma_{11}^2 = \frac{1}{J} \frac{\partial^2 x^2}{\partial (\xi^1)^2} = \frac{1}{1 + \eta_1} \left(\xi^2 \frac{\partial^2 \eta_1}{\partial (\xi^1)^2} + \frac{\partial^2 \eta_0}{\partial (\xi^1)^2} \right),$$

$$\Gamma_{12}^2 = \Gamma_{21}^2 = \frac{1}{J} \frac{\partial^2 x^2}{\partial \xi^1 \partial \xi^2} = \frac{1}{1 + \eta_1} \frac{\partial \eta_1}{\partial \xi^1}.$$

To simplify the notation, we define the following non-constant transformation coefficients

$$\varphi_1 = \frac{\partial \xi^2}{\partial x^1} = -\frac{1}{J} \frac{\partial x^2}{\partial \xi^1} = -\frac{1}{1 + \eta_1} \left(\xi^2 \frac{\partial \eta_1}{\partial \xi^1} + \frac{\partial \eta_0}{\partial \xi^1} \right),$$

$$\varphi_2 = \frac{\partial \xi^2}{\partial x^2} = \frac{1}{J} = \frac{1}{1 + \eta_1},$$

$$\varphi_\tau = \frac{\partial \xi^2}{\partial t} = -\frac{1}{J} \frac{\partial x^2}{\partial \tau} = -\frac{1}{1 + \eta_1} \left(\xi^2 \frac{\partial \eta_1}{\partial \tau} + \frac{\partial \eta_0}{\partial \tau} \right).$$

The two components of the momentum Eq. (28) may be written, after some manipulations, as

$$\begin{aligned} \frac{\partial u^1}{\partial \tau} + \varphi_\tau \frac{\partial u^1}{\partial \xi^2} + u^1 \frac{\partial u^1}{\partial \xi^1} + u^2 \frac{\partial u^1}{\partial \xi^2} &= -\frac{1}{\rho} \left(\frac{\partial p}{\partial \xi^1} + \varphi_1 \frac{\partial p}{\partial \xi^2} \right) \\ &+ v \left[\left(\frac{\partial}{\partial \xi^1} + \varphi_1 \frac{\partial}{\partial \xi^2} \right) \left(\frac{\partial}{\partial \xi^1} + \varphi_1 \frac{\partial}{\partial \xi^2} \right) u^1 + \varphi_2^2 \frac{\partial^2 u^1}{\partial (\xi^2)^2} \right] - P_x, \end{aligned}$$

$$\begin{aligned}
 & \frac{\partial u^2}{\partial \tau} + \varphi_\tau \frac{\partial u^2}{\partial \xi^2} - \underbrace{u^1 \frac{\partial \varphi_\tau}{\partial \xi^1} - u^2 \frac{\partial \varphi_\tau}{\partial \xi^2}} + u^1 \frac{\partial u^2}{\partial \xi^1} + u^2 \frac{\partial u^2}{\partial \xi^2} + u^1 u^2 \frac{2}{J} \frac{\partial J}{\partial \xi^1} + u^1 u^1 \frac{1}{J} \frac{\partial^2 x^2}{\partial (\xi^1)^2} \\
 & = -\frac{1}{\rho} \varphi_1 \left(\frac{\partial p}{\partial \xi^1} + \varphi_1 \frac{\partial p}{\partial \xi^2} \right) - \frac{1}{\rho} \varphi_2^2 \frac{\partial p}{\partial \xi^2} - \varphi_1 P_x + \nu \varphi_2 \left[\left(\frac{\partial}{\partial \xi^1} + \varphi_1 \frac{\partial}{\partial \xi^2} \right) \left(\frac{\partial}{\partial \xi^1} + \varphi_1 \frac{\partial}{\partial \xi^2} \right) (Ju^2) \right. \\
 & \quad \left. + \varphi_2^2 \frac{\partial^2 Ju^2}{\partial (\xi^2)^2} + u^1 s_1 + 2 \frac{\partial u^1}{\partial \xi^1} s_2 + 2 \frac{\partial u^1}{\partial \xi^2} s_3 \right], \tag{35}
 \end{aligned}$$

where ν is the kinematic viscosity, P_x is the uniform streamwise (x^1 -direction) pressure gradient that maintains the bulk flow, and

$$s_1 = \left(\frac{\partial}{\partial \xi^1} + \varphi_1 \frac{\partial}{\partial \xi^2} \right) s_2,$$

$$s_2 = \frac{\partial^2 x^2}{\partial (\xi^1)^2} + \varphi_1 \frac{\partial J}{\partial \xi^1},$$

$$s_3 = \varphi_1 s_2 + \varphi_2^2 \frac{\partial J}{\partial \xi^1}.$$

By applying the metric invariants of the coordinate transformation, we may also express the conservative form of the momentum equation (see Appendix, Eq. (A.1)), which is preferable for implementation in a numerical algorithm.

In the particular transformation shown above, applying (9) would cause the two under-braced terms $-u^1 \frac{\partial \varphi_\tau}{\partial \xi^1} - u^2 \frac{\partial \varphi_\tau}{\partial \xi^2}$ in the u^2 momentum equation in (35) to be absent. The continuity equation and boundary conditions are given in the Appendix.

4.1. Numerical algorithm

To solve (35), the volume flux components $q^1 = Ju^1$, $q^2 = Ju^2$, and the modified pressure $\bar{p} = Jp/\rho$ are chosen as the primitive variables. The numerical algorithm is based on that in [21,22]. The grid is chosen to be evenly spaced in the streamwise direction (ξ^1) and non-staggered so that Fourier transformation techniques may be used to compute spatial derivatives in this direction. In the wall-normal direction (ξ^2) the grid is staggered and stretched using a hyperbolic tangent function allowing the near-wall region to be better resolved. Spatial derivatives of this direction is discretized using the second order centered finite difference scheme.

The flow is advanced in time using a low-storage third-order Runge–Kutta method. At each Runge–Kutta substep, all terms involving ξ^1 derivatives and cross derivatives of the primitive variables are treated explicitly, and all terms involving only ξ^2 derivatives of the primitive variables are treated with an implicit Crank–Nicholson method.

At the beginning of a time step, a full pressure equation is solved with a Neumann boundary condition that is derived by imposing the discrete continuity constraint upon the discrete momentum equation. At the end of each Runge–Kutta substep, a projection function is solved to bring the velocity field to be solenoidal and to update the pressure. Readers are referred to the Appendix for the details of this numerical method.

To maintain the constant bulk velocity U_{bulk} (which is normalized by the nominal domain size), the uniform streamwise pressure gradient P_x is computed by integrating the u^1 momentum equation over the entire domain,

$$\begin{aligned}
 U_{\text{bulk}} &= \frac{1}{2L_x} \int_{-1+\eta_l}^{1+\eta_u} \int_0^{L_x} v^1 dx^1 dx^2 = \text{constant} \\
 \Rightarrow P_x &= \frac{1}{2 \int J d\xi^1} \int \left[-\varphi_1 \bar{p} + v\varphi_1 \frac{\partial \varphi_1 q^1}{\partial \xi^2} + v\varphi_2^2 \frac{\partial q^1}{\partial \xi^2} \right]_{\xi^2=-1}^{\xi^2=1} d\xi^1.
 \end{aligned} \tag{36}$$

The discrete numerical integration scheme in the code exactly conserves both mass and momentum. By computing P_x with (36), constant mass flux is numerically guaranteed. The Reynolds number is thus based on the bulk volume flux

$$Re = \frac{U_c h}{\nu} = \frac{3}{2} \frac{U_{\text{bulk}} h}{\nu},$$

where $U_c = \frac{3}{2} U_{\text{bulk}}$ is the centerline velocity of the corresponding Poiseuille flow with the same mass flux, and $h = 1$ is the half channel width. Time is normalized by $\frac{h}{U_c}$.

4.2. Laminar steady flow in channels with sinusoidal walls

The first case considered is the laminar flow in a symmetric channel with sinusoidal walls, as depicted in Fig. 1, with $\eta_l = -\eta_u = \varepsilon \cos(\xi^1)$. This case, though not addressing the problem of a moving coordinate system, validates the correctness of the present code against an analytic result in the case of a stationary coordinate system. The parabolic laminar profile in an unperturbed channel is used as the initial condition. The wall deformation starts to grow gradually until the final geometry is reached and then remains unchanged, and the simulation continues until the steady state is reached. The results are compared with that from Tsangaris and Leiter [23], who solved the laminar steady flow in sinusoidal channels for Reynolds numbers far above that for creeping flow. In their work, a perturbation method is used with the wall amplitude ε as the perturbation parameter. The stream function is expanded in a series, and the first-order variation is derived, which boils down to solving numerically a linear system of 4th-order differential equations with two unknown functions and with variable coefficients.

Figs. 2 and 3 show the comparison of the Cartesian velocity components (v^1 and v^2) profiles for $\varepsilon = 0.1$ and $\varepsilon = 0.2$ at Reynolds numbers $Re = 1.0, 10, 75, 200, 400$. In our simulations, the number of Fourier modes is 32×64 in the ξ^1 and ξ^2 directions, respectively (i.e., 48×64 dealiased collocation points), and the length of the computational domain is $L_x = 2\pi$. The resolution was doubled in both directions and the calculations repeated with no significant change of the results.

The comparisons show that our simulations agree very well with the results obtained by Tsangaris and Leiter when both the wall deformation parameter ε and the Reynolds number Re are small. However, the discrepancies become more evident as ε or Re is increased. The influence of ε is expected because the perturbation analysis of Tsangaris and Leiter is less accurate when the perturbation parameter ε is increased. The influence of Re is also expected since the leading-order truncation error from the perturbation series is related to Reynolds number as well.

Our simulations also show that the critical Reynolds number for flow separation to happen at $\varepsilon = 0.2$ is about $Re_{\text{crit}} = 171$, and the separation point is about $\xi^1 = 2.6$ which is slightly upstream the maximum width of the wavy wall of the channel. These are slightly different from what Tsangaris and Leiter predicted, where $Re_{\text{crit}} = 185$ and the separation point is about $\xi^1 = 2.4$. As Reynolds number is increased above Re_{crit} , separation regions in the diverging portion of the channel are formed, as illustrated in Fig. 4.

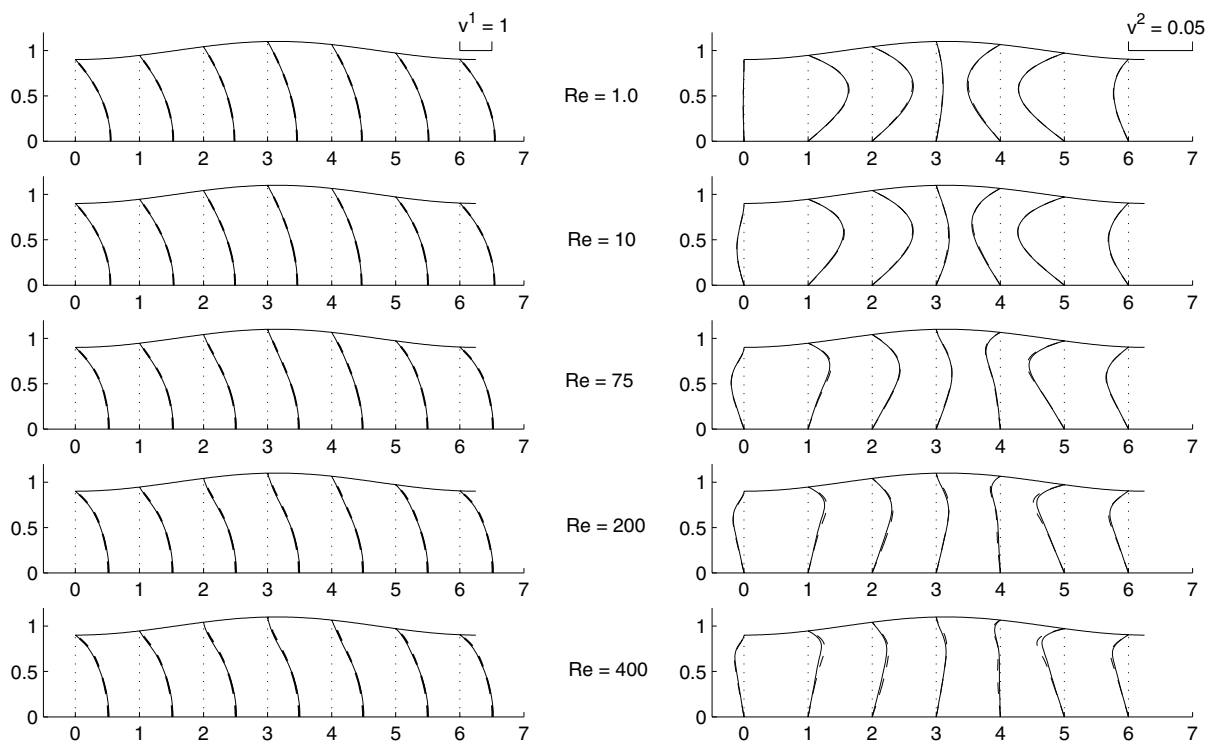


Fig. 2. Cartesian velocity profiles at various cross sections ($x^1 = 0, 1, 2, 3, 4, 5, 6$) of the channel for steady flow with $\varepsilon = 0.1$ and various Reynolds numbers. Left: v^1 component; Right: v^2 component. Solid: numerical results; dashed: perturbation analysis.

4.3. Moving boundary simulation

To illustrate the important effects of the sometimes-neglected terms in the Navier–Stokes equations in time-dependent curvilinear coordinates, we simulate the laminar flow in a channel with an oscillating Gaussian protuberance at center of the lower wall and corresponding blowing/suction applied at the opposite wall. The wall deformation is prescribed by

$$\eta_l(\xi^1, t) = \varepsilon \sin(\omega t) \exp \left[-\frac{(\xi^1 - \frac{L_x}{2})^2}{\sigma^2} \right],$$

where ε is the amplitude of the wall deformation, ω is the oscillation frequency, and σ is a constant determining the width of the protuberance.

To maintain the incompressibility of the flow, the upper wall is made porous and the velocity of the fluid through the upper wall is identical to the velocity of the lower wall. In all tests of this section, the channel length is chosen to be $L_x = \pi$, Reynolds number is $Re = 200$, and the wall deformation parameters are $\varepsilon = 0.1$ and $\sigma = 0.2$. In the simulation, the number of Fourier modes is 42×84 in the ξ^1 and ξ^2 directions respectively (i.e., 64×84 dealiased collocation points) and the time step is 0.01. The time step was reduced by a factor of 10 and there was no significant change of the results.

Due to the oscillation of the boundary, this flow exhibits time-periodic behavior. Fig. 5 shows both the instantaneous streamlines' and pressure's oscillating patterns at different time phases within one period

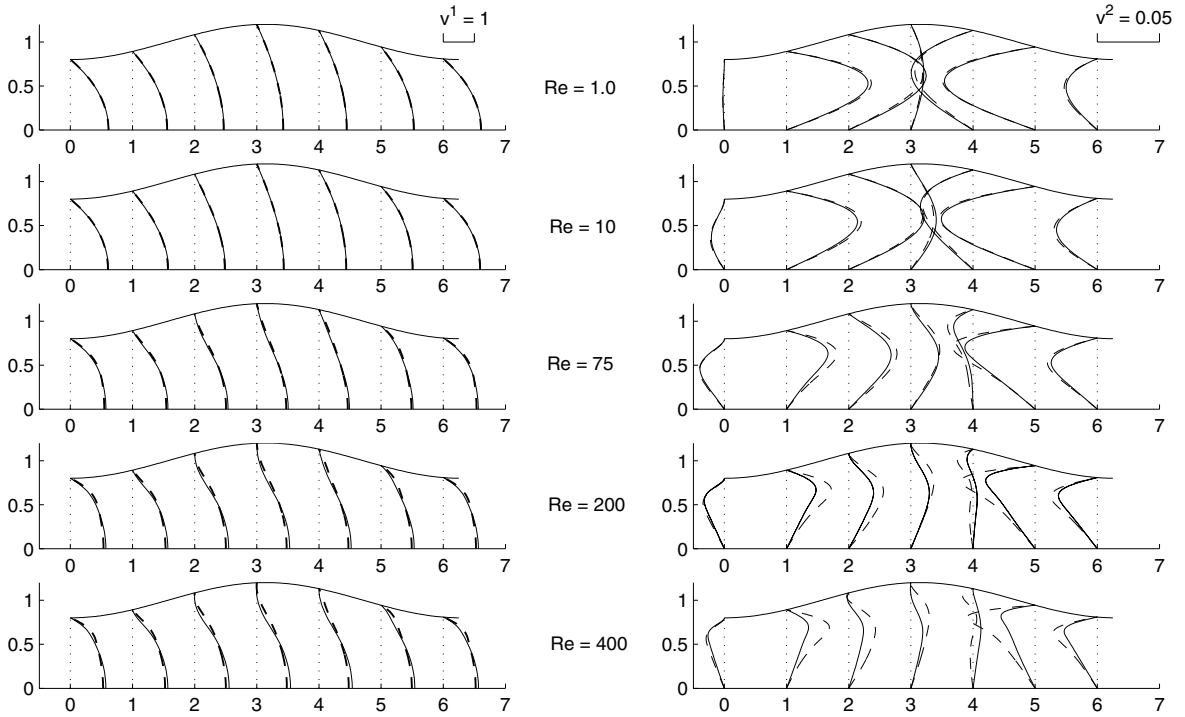


Fig. 3. Cartesian velocity profiles at various cross sections ($x^1 = 0, 1, 2, 3, 4, 5, 6$) of the channel for steady flow with $\varepsilon = 0.2$ and various Reynolds numbers. Left: v^1 component; Right: v^2 component. Solid: numerical results; dashed: perturbation analysis.

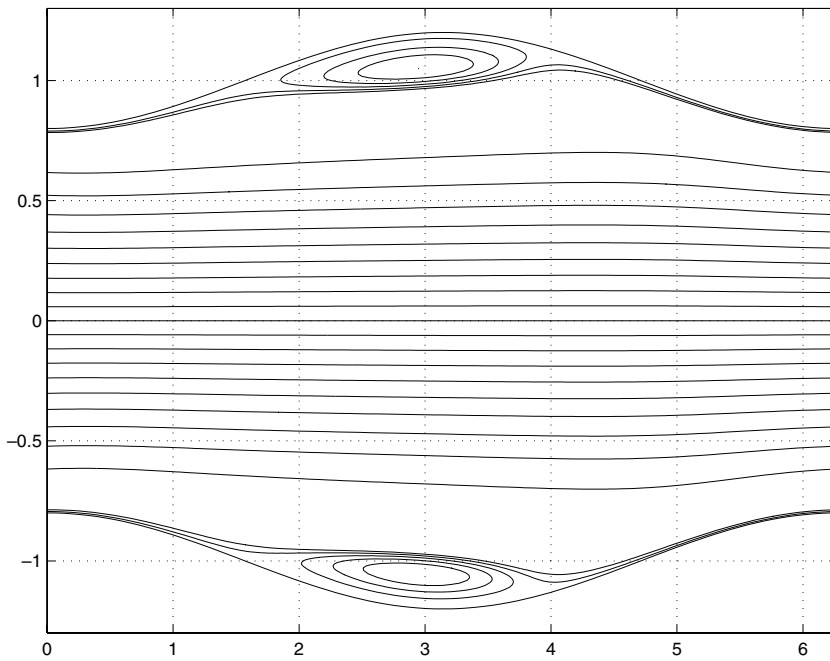


Fig. 4. The streamlines for the case with $\varepsilon = 0.2$ and $Re = 400$ showing the separation regions of the flow field.

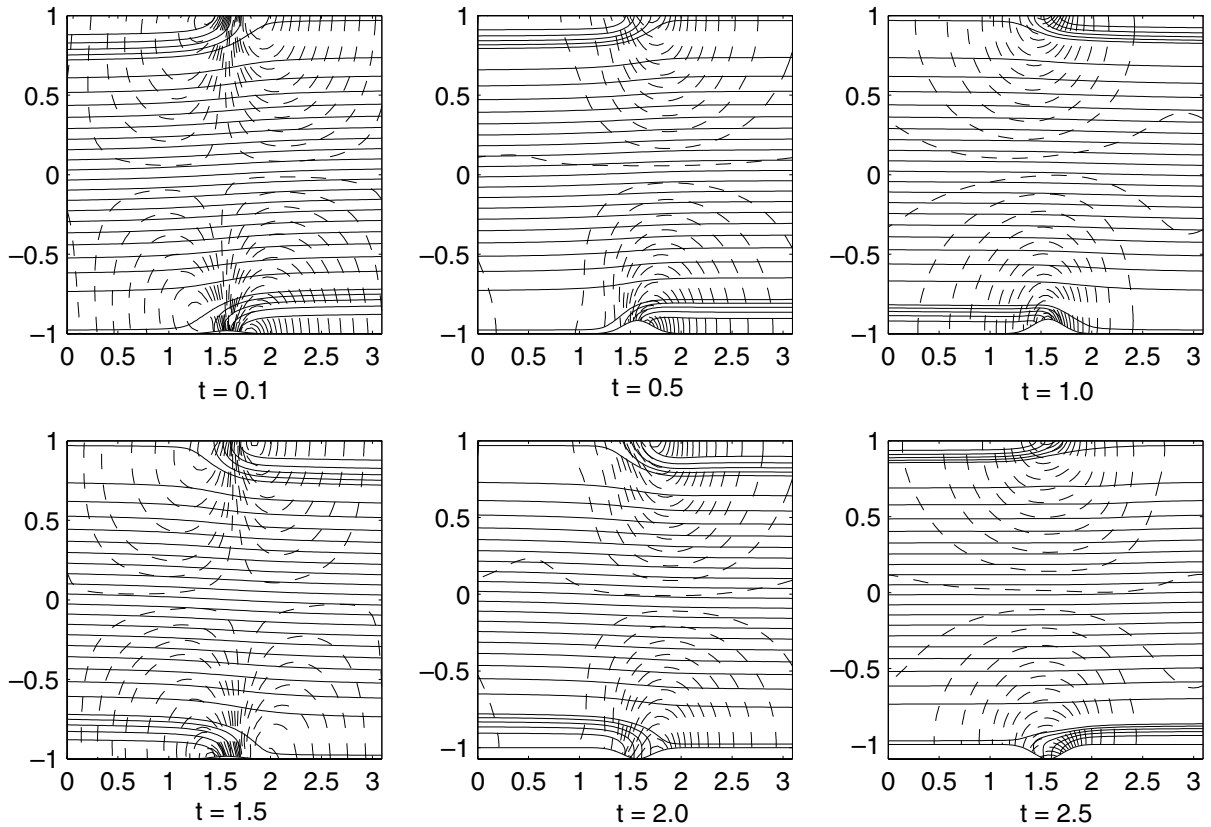


Fig. 5. Instantaneous streamlines (solid) and pressure (dashed) contours within one cycle of flow of $Re = 200$ in a channel with an oscillating Gaussian protuberance on the lower wall and corresponding blowing/suction on the upper wall. In all figures, the flow goes from left to right.

cycle $\frac{2\pi}{\omega} = \pi$ (i.e., $\omega = 2$). The streamline patterns show that center of the two walls serves as the fluid source or sink in the transversal direction of the flow. Whenever the lower wall is moving upward, serving as a source (i.e., $t = 0.1, 0.5, 2.5$), the instantaneous streamlines near the wall are combed downstream, which means the fluid is pushed up by the wall and drifts downstream with the main flow, and at the upper wall region, the instantaneous streamlines are contracted toward the wall by the corresponding fluid extraction. By similar reasoning, when the lower wall is moving downward, serving as a sink (i.e., $t = 1.0, 1.5, 2.0$), the instantaneous streamline patterns near the lower wall and the upper wall reverse. The pressure patterns oscillate in time as well. At $t = 0.1$, a high-pressure region is formed at the front side of the bump due to the interaction between the viscous fluid and the rising obstacle, and a low pressure region is formed at the back. Form drag is therefore introduced in addition to the skin friction. The high pressure region gradually fades and the low pressure region shifts upstream as the bump descends ($t = 0.5$ and $t = 1.0$). When the wall moves down farther ($t = 1.5$), the low pressure region shifts to the upstream side of the bump and another high pressure region is formed downstream. Then the low pressure region gradually fades and the high pressure region shifts upstream ($t = 2.0$ and $t = 2.5$).

We also simulated the flow with under-braced terms in Eq. (35) intentionally omitted in the code. Since these terms arise from the temporal derivative, we may expect that the errors associated with their omission

would be small if the wall motion is slow, but large if the wall motion is fast. Two comparisons are carried out, one with oscillation frequency $\omega = 0.5$, the other with $\omega = 4$. The resulting instantaneous streamlines and pressure contours at a phase of the oscillation are shown in Figs. 6 and 7. In the slow wall motion case, $\omega = 0.5$, the calculations with the terms omitted approximate our correct results fairly well. However, in the faster wall motion case, $\omega = 4$, the effects of omitted terms in the calculations become more evident. In Fig. 7, where the wall is moving upward, the streamlines appear to overshoot above the bump, and undershoot downstream due to this omission. The pressure contours also become more irregular when the two terms are absent from the calculation.

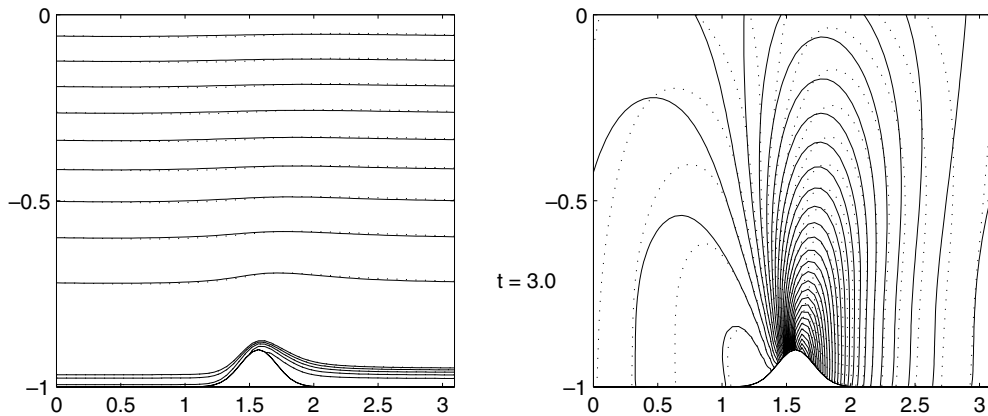


Fig. 6. Effects of the sometimes-neglected terms in the Navier–Stokes equations on flow of $Re = 200$ when wall oscillation is slow ($\omega = 0.5$). Time instance: $t = 3.0$. Left: instantaneous streamlines ψ ; Right: pressure contours. Solid: the correct results; dotted: results with neglected terms. Quantification of error: $\|\psi_{\text{error}}\|_2/\|\psi\|_2 = 0.2\%$; $\max_{\Omega}(\psi_{\text{error}})/\|\psi\|_2 = 0.5\%$; $\|p_{\text{error}}\|_2/\|p\|_2 = 17\%$; $\max_{\Omega}(p_{\text{error}})/\|p\|_2 = 35\%$.

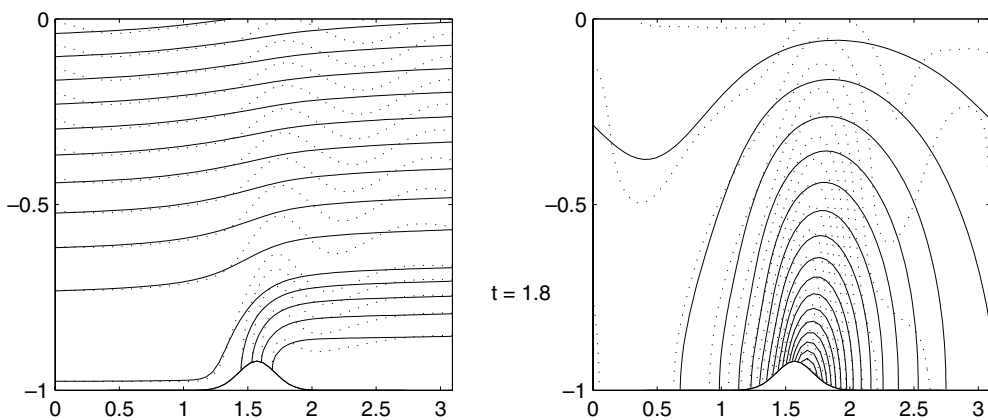


Fig. 7. Effects of the sometimes-neglected terms in the Navier–Stokes equations on flow of $Re = 200$ when wall oscillation is fast ($\omega = 4$). Time instance: $t = 1.8$. Left: instantaneous streamlines ψ ; Right: pressure contours. Solid: the correct results; dotted: results with neglected terms. Quantification of error: $\|\psi_{\text{error}}\|_2/\|\psi\|_2 = 1.6\%$; $\max_{\Omega}(\psi_{\text{error}})/\|\psi\|_2 = 6.8\%$; $\|p_{\text{error}}\|_2/\|p\|_2 = 15\%$; $\max_{\Omega}(p_{\text{error}})/\|p\|_2 = 55\%$.

5. Conclusions

In time-dependent curvilinear coordinates, the temporal derivative of a tensor vector is more complicated than the temporal derivative of a scalar. From Eq. (23), we can see that, for a contravariant vector A^j , its temporal intrinsic derivative involves its own covariant differentiation ($A^j_{;i}U^i$) and the covariant differentiation of the velocity of the coordinates ($A^iU^j_{;i}$). Treating A^j as a scalar during time differentiation is incorrect, as it drops some important terms. Since $U^j_{;i} = \bar{c}^j_i \frac{\partial c^i_j}{\partial \tau}$ as we have shown, and $c^i_j = \frac{\partial x^i}{\partial \bar{x}^j}$ is actually the component of the base vectors of the new coordinate system, the term $A^iU^j_{;i}$ arises because base vectors of the new coordinates are moving. Generally, in a time-dependent coordinate system $A^iU^j_{;i}$ would not vanish even if the coordinate lines are straight and/or orthogonal, as shown by the two examples in Sections 2.4 and 2.5.

Assuming that the extra terms in question are small is only valid when the coordinate system is moving sufficiently slowly. We have demonstrated that these terms are not always negligible by simulating incompressible flows in a two-dimensional channel with prescribed boundary motion.

Acknowledgements

The authors would like to thank Prof. Constantine Pozrikidis of UC, San Diego for his valuable suggestions and comments during the course of this work.

Appendix A. Numerical implementation

In primitive variables. i.e., the volume flux components $q^1 = Ju^1$, $q^2 = Ju^2$, and the modified pressure $\bar{p} = Jp/\rho$, the conservative form of governing Eq. (35) for the compliant channel can be written as

$$\frac{\partial q^i}{\partial \tau} + T^i(q^j) + N^i(q^j) = -G^i(\bar{p}) + \nu L^i(q^j) - P^i, \tag{A.1}$$

where $T^i(q^j)$ is the term involving φ_τ , $N^i(q^j)$ is the convection term, $G^i(\bar{p})$ is the pressure gradient term, $\nu L^i(q^j)$ is the diffusion term, and P^i is the uniform pressure gradient term. They are given by

$$T^1 = \frac{\partial q^1 \varphi_\tau}{\partial \xi^2},$$

$$T^2 = \frac{\partial q^2 \varphi_\tau}{\partial \xi^2} - q^1 \frac{\partial \varphi_\tau}{\partial \xi^1} - q^2 \frac{\partial \varphi_\tau}{\partial \xi^2},$$

$$N^1 = \frac{\partial q^1 q^1 \varphi_2}{\partial \xi^1} + \frac{\partial q^1 q^2 \varphi_2}{\partial \xi^2},$$

$$N^2 = \frac{\partial q^1 q^2 \varphi_2}{\partial \xi^1} + \frac{\partial q^2 q^2 \varphi_2}{\partial \xi^2} + 2\varphi_2 q^1 q^2 \frac{\partial J}{\partial \xi^1} + \varphi_2 q^1 q^1 \frac{\partial^2 x^2}{\partial (\xi^1)^2},$$

$$G^1 = \frac{\partial \bar{p}}{\partial \xi^1} + \frac{\partial \bar{p} \varphi_1}{\partial \xi^2},$$

$$G^2 = \varphi_1 \left(\frac{\partial \bar{p}}{\partial \xi^1} + \frac{\partial \bar{p} \varphi_1}{\partial \xi^2} \right) + \varphi_2^2 \frac{\partial \bar{p}}{\partial \xi^2},$$

$$L^1 = \left(\frac{\partial}{\partial \xi^1} + \frac{\partial \varphi_1}{\partial \xi^2} \right) \left(\frac{\partial}{\partial \xi^1} + \frac{\partial \varphi_1}{\partial \xi^2} \right) (q^1) + \varphi_2^2 \frac{\partial^2 q^1}{\partial (\xi^2)^2},$$

$$L^2 = \left(\frac{\partial}{\partial \xi^1} + \varphi_1 \frac{\partial}{\partial \xi^2} \right) \left(\frac{\partial}{\partial \xi^1} + \varphi_1 \frac{\partial}{\partial \xi^2} \right) (q^2) + \varphi_2^2 \frac{\partial^2 q^2}{\partial (\xi^2)^2} + \varphi_2 q^1 s_1 + 2 \frac{\partial \varphi_2 q^1}{\partial \xi^1} s_2 + 2 \frac{\partial \varphi_2 q^1}{\partial \xi^2} s_3,$$

$$P^1 = J P_x,$$

$$P^2 = J \varphi_1 P_x.$$

Weighted by J , the continuity equation is

$$D_i q^i = \frac{\partial q^1}{\partial \xi^1} + \frac{\partial q^2}{\partial \xi^2} = 0, \quad (\text{A.2})$$

where D_i is the divergence operator. The boundary conditions are the no-slip and no-penetration boundary conditions which can be expressed as

$$\begin{aligned} q^1|_{\xi^2=\pm 1} &= 0, \\ q^2|_{\xi^2=+1} &= \frac{\partial \eta_u}{\partial \tau}, \\ q^2|_{\xi^2=-1} &= \frac{\partial \eta_l}{\partial \tau}. \end{aligned} \quad (\text{A.3})$$

One exception in present work is the example of moving boundary with Gaussian protuberance where the upper wall is made porous and the boundary condition for the upper wall is thus $q^2|_{\xi^2=+1} = q^2|_{\xi^2=-1} = \frac{\partial \eta}{\partial \tau}$.

A.1. Temporal discretization

The flow is marched in time with a low-storage third-order Runge–Kutta method based on the scheme used by Akselvoll and Moin [21] and Bewley et al. [22]. In each of the three Runge–Kutta substeps $k = 1, 2, 3$, two fractional steps are used: (1) an intermediate flow field q^{i*} is obtained by solving the momentum equation with some terms treated explicitly and some implicitly (Crank–Nicholson); (2) the velocities q^{i*} are projected to the divergence free space and the pressure is updated by the projection function.

Let the operator A_i represent the terms treated explicitly and B_i represent the terms treated implicitly where the subscripts simply indicate the operator components, not covariant components. The discretized momentum equation may be written as

$$\frac{q^{i*} - q^{i^{k-1}}}{\delta \tau} = \beta_k \left(B_i(q^{i*}) + B_i(q^{i^{k-1}}) \right) + \gamma_k A_i(q^{i^{k-1}}) + \zeta_k A_i(q^{i^{k-2}}) + 2\beta_k \left(G^i(\bar{p}^{k-1}) - P^i \right), \quad (\text{A.4})$$

where the explicit and implicit operators are given by

$$A_1(q^j) = v \frac{\delta}{\delta \xi^1} \left(\frac{\delta q^1}{\delta \xi^1} + \frac{\delta \varphi_1 q^1}{\delta \xi^2} \right) + v \frac{\delta}{\delta \xi^2} \left(\varphi_1 \frac{\delta q^1}{\delta \xi^1} \right) - \frac{\delta q^1 q^1 \varphi_2}{\delta \xi^1},$$

$$A_2(q^j) = v \frac{\delta}{\delta \xi^1} \left(\frac{\delta q^2}{\delta \xi^1} + \varphi_1 \frac{\delta q^2}{\delta \xi^2} \right) + v \varphi_1 \frac{\delta}{\delta \xi^2} \left(\frac{\delta q^2}{\delta \xi^1} \right) + v \left(\varphi_2 q^1 s_1 + 2 \frac{\partial \varphi_2 q^1}{\partial \xi^1} s_2 + 2 \frac{\partial \varphi_2 q^1}{\partial \xi^2} s_3 \right) - \frac{\delta q^1 q^2 \varphi_2}{\delta \xi^1} - \varphi_2^2 q^1 q^1 \frac{\delta}{\delta \xi^1} \left(\frac{\delta x^2}{\delta \xi^1} \right) + q^1 \frac{\delta \varphi_\tau}{\delta \xi^1},$$

$$B_1(q^j) = v \frac{\delta}{\delta \xi^2} \left(\varphi_1 \frac{\delta \varphi_1 q^1}{\delta \xi^2} \right) + v \varphi_2^2 \frac{\delta}{\delta \xi^2} \left(\frac{\delta q^1}{\delta \xi^2} \right) - \frac{\delta q^1 q^2 \varphi_2}{\delta \xi^2} - \frac{\delta q^1 \varphi_\tau}{\delta \xi^2},$$

$$B_2(q^j) = v \varphi_1 \frac{\delta}{\delta \xi^2} \left(\varphi_1 \frac{\delta q^2}{\delta \xi^2} \right) + v \varphi_2^2 \frac{\delta}{\delta \xi^2} \left(\frac{\delta q^2}{\delta \xi^2} \right) - \frac{\delta q^2 q^2 \varphi_2}{\delta \xi^2} - 2 \varphi_2^2 q^1 q^2 \frac{\delta J}{\delta \xi^1} - \frac{\delta q^2 \varphi_\tau}{\delta \xi^2} + q^2 \frac{\delta \varphi_\tau}{\delta \xi^2},$$

and $\frac{\delta}{\delta \xi^i}$ means the numerical differentiation. The Runge–Kutta coefficients used in the present computations are:

$$\begin{aligned} \beta_1 &= \frac{4}{15}, & \beta_2 &= \frac{1}{15}, & \beta_3 &= \frac{1}{6}, \\ \gamma_1 &= \frac{8}{15}, & \gamma_2 &= \frac{5}{12}, & \gamma_3 &= \frac{3}{4}, \\ \zeta_1 &= 0, & \zeta_2 &= -\frac{17}{60}, & \zeta_3 &= -\frac{5}{12}. \end{aligned}$$

Note that, in the same way as in [21], the non-linear term $q^2 q^2$ needs to be linearized for the present system to be solvable.

To make the intermediate flow field divergence free, we solve a projection function for $\phi = \bar{p}^k - \bar{p}^{k-1}$:

$$\Delta \phi = \frac{1}{2\beta_k \delta \tau} \frac{\delta q^{i*}}{\delta \xi^i},$$

where Δ is the Laplacian operator given by

$$\Delta \phi = D_i G^i(\phi) = \frac{\delta}{\delta \xi^1} \left(\frac{\delta \phi}{\delta \xi^1} + \frac{\delta \phi \varphi_1}{\delta \xi^2} \right) + \frac{\delta}{\delta \xi^2} \left[\varphi_1 \left(\frac{\delta \phi}{\delta \xi^1} + \frac{\delta \phi \varphi_1}{\delta \xi^2} \right) \right] + \varphi_2^2 \frac{\delta}{\delta \xi^2} \left(\frac{\delta \phi}{\delta \xi^2} \right). \tag{A.5}$$

This Poisson equation is solved in Fourier space. Since the non-constant coefficients make the Laplacian non-invertible, we split the operator into two parts and solve the equation iteratively,

$$\tilde{\Delta} \phi^s = \frac{\delta}{\delta \xi^i} \left(\frac{\delta \phi^s}{\delta \xi^i} \right) = \text{RHS}^{s-1} = \frac{1}{2\beta_k \delta \tau} \frac{\delta q^{i*}}{\delta \xi^i} - (\Delta - \tilde{\Delta})(\phi^{s-1}), \tag{A.6}$$

where s is the iteration index. After ϕ converges, the volume flux components and pressure are updated by

$$q^k = q^{i*} - 2\beta_k \delta \tau G^i(\phi) \tag{A.7}$$

and

$$\bar{p}^k = \bar{p}^{k-1} + \phi. \tag{A.8}$$

A.2. Pressure equation

At the beginning of each time step, we solve a full pressure equation which is obtained by taking divergence of the Eq. (A.1):

$$\Delta \bar{p} = D_i(-T^i - N^i + \nu L^i). \quad (\text{A.9})$$

Note that the divergence of the uniform pressure gradient vanishes, which is true (within the machine accuracy) in the discrete case as well. The Laplacian Δ is the same as in (A.5), so the pressure equation is solved with the same iteration strategy as that used in (A.6).

The grid is discretized with a hyperbolic tangent stretching function and staggered in the wall-normal direction. q^2 is assigned on the family of gridpoints $j = 0, 1, 2, \dots$, where $j = 0$ corresponds to the lower wall, and q^1, \bar{p} are assigned on the family of gridpoints $j = \frac{1}{2}, 1 + \frac{1}{2}, 2 + \frac{1}{2}, \dots$, where $j = \frac{1}{2}$ is midway between $j = 0$ and $j = 1$, and so on. Neumann boundary conditions for pressure are derived by enforcing continuity of the flow at the first interior gridpoint. We illustrate the procedure for the lower wall, $\zeta^2 = -1$.

The discrete q^1 momentum at $j = \frac{1}{2}$ and the discrete q^2 momentum at $j = 1$, in an explicit Euler scheme, may be written as

$$\begin{aligned} \left. \frac{q^{1*} - q^{1^{k-1}}}{2\beta_k \delta\tau} \right|_{j=\frac{1}{2}} &= (-T^1 - N^1 - G^1 + \nu L^1 - P^1)|_{j=\frac{1}{2}} \\ \left. \frac{q^{2*} - q^{2^{k-1}}}{2\beta_k \delta\tau} \right|_{j=1} &= (-T^2 - N^2 - G^2 + \nu L^2 - P^2)|_{j=1}, \end{aligned} \quad (\text{A.10})$$

and the boundary condition for q^{2*} is

$$q^{2*}|_{j=0} = q^{2^k}|_{j=0}. \quad (\text{A.11})$$

Applying the discrete divergence operator to \mathbf{q}^* at $j = \frac{1}{2}$, that is,

$$(D_i q^{i*})|_{j=\frac{1}{2}} = \frac{\delta q^{1*}|_{j=\frac{1}{2}}}{\delta \zeta^1} + \frac{1}{h_{\frac{1}{2}}} (q^{2*}|_{j=1} - q^{2*}|_{j=0}),$$

where $h_{\frac{1}{2}}$ is the distance between gridpoints $j = 0$ and $j = 1$, and requiring it to be zero, we have

$$\begin{aligned} & -\frac{1}{2\beta_k \delta\tau} \left(\frac{\delta q^{1^{k-1}}|_{j=\frac{1}{2}}}{\delta \zeta^1} + \frac{q^{2^{k-1}}|_{j=1} - q^{2^{k-1}}|_{j=0}}{h_{\frac{1}{2}}} \right) + \frac{1}{2\beta_k \delta\tau} \left(\frac{q^{2^k}|_{j=0} - q^{2^{k-1}}|_{j=0}}{h_{\frac{1}{2}}} \right) \\ &= \frac{\delta}{\delta \zeta^1} (-T^1 - N^1 - G^1 + \nu L^1 - P^1)|_{j=\frac{1}{2}} + \frac{1}{h_{\frac{1}{2}}} [(-T^2 - N^2 - G^2 + \nu L^2 - P^2)|_{j=1} \\ & \quad + (N^2 + G^2)|_{j=0} - (N^2 + G^2)|_{j=0}], \end{aligned} \quad (\text{A.12})$$

where the boundary nodes $q^{2^{k-1}}|_{j=0}$ and $(N^2 + G^2)|_{j=0}$ have been introduced. Note that the expression in the first parentheses on the left hand side vanishes since \mathbf{q}^{k-1} is divergence free. We split (A.12) into two equations:

$$0 = \frac{\delta}{\delta \zeta^1} (-N^1 - G^1)|_{j=\frac{1}{2}} + \frac{1}{h_{\frac{1}{2}}} [(-N^2 - G^2)|_{j=1} + (N^2 + G^2)|_{j=0}], \quad (\text{A.13})$$

$$\left. \frac{q^{2k} - q^{2k-1}}{2\beta_k \delta\tau} \right|_{j=0} + \left(h_{\frac{1}{2}} \frac{\delta T^1|_{j=\frac{1}{2}}}{\delta\xi^1} + T^2|_{j=1} \right) + N^2|_{j=0} = -(G^2 + P^2)|_{j=0} + v \left(h_{\frac{1}{2}} \frac{\delta L^1|_{j=\frac{1}{2}}}{\delta\xi^1} + L^2|_{j=1} \right), \quad (\text{A.14})$$

where $h_{\frac{1}{2}} \frac{\delta P^1|_{j=\frac{1}{2}}}{\delta\xi^1} + P^2|_{j=1} = P^2|_{j=0}$ has been applied since P^i is divergence free. Note that (A.13) has the form of the simplified pressure equation, so it may be treated as the Poisson equation (A.9) evaluated at $j = \frac{1}{2}$. Eq. (A.14) may be used to compute $G^2|_{j=0}$ which is the Neumann boundary condition for (A.9). Actually, by realizing that in theory T^i and L^i are divergence free, we have

$$h_{\frac{1}{2}} \frac{\delta T^1|_{j=\frac{1}{2}}}{\delta\xi^1} + T^2|_{j=1} \approx T^2|_{j=0}, \quad h_{\frac{1}{2}} \frac{\delta L^1|_{j=\frac{1}{2}}}{\delta\xi^1} + L^2|_{j=1} \approx L^2|_{j=0}.$$

Therefore, (A.14) is essentially the q^2 momentum equation evaluated at the lower boundary.

References

- [1] R. Aris, Vectors, Tensors, and the Basic Equations of Fluid Mechanics, Prentice-Hall, Englewood Cliffs, NJ, 1962.
- [2] P.D. Thomas, C.K. Lombard, Geometric conservation law and its application to flow computations on moving grids, *AIAA J.* 17 (10) (1979) 1030–1037.
- [3] R. Hixon, Numerically consistent strong conservation grid motion for finite difference schemes, *AIAA J.* 38 (9) (2000) 1586–1593.
- [4] T.H. Pulliam, J.L. Steger, Implicit finite-difference simulations of three dimensional compressible flow, *AIAA J.* 18 (2) (1980) 159–167.
- [5] R. Smith, W. Shyy, Computation of unsteady laminar flow over a flexible two-dimensional membrane wing, *Phys. Fluids* 7 (9) (1995) 2175–2184.
- [6] C. Sheng, L.K. Taylor, D. Whitfield, Multigrid algorithm for three dimensional incompressible high-reynolds number turbulent flows, *AIAA J.* 33 (11) (1995) 2073–2079.
- [7] Z. Lei, G. Liao, G.C. dela Pena, A moving grid algorithm based on the deformation method. In: Nobuyuki Satofuka (Ed.), *Computational Fluid Dynamics 2000: Proceedings of the First International Conference on Computational Fluid Dynamics, ICCFD, Kyoto, Japan, July 10–14, 2000*, Springer-Verlag, New York, 2001, pp. 711–716.
- [8] B.R. Hodges, R.L. Street, On simulation of turbulent nonlinear free-surface flows, *J. Comput. Phys.* 151 (1999) 425–457.
- [9] P.R. Voke, M.W. Collins, Forms of the generalized Navier–Stokes equations, *J. Eng. Math.* 18 (1984) 219–233.
- [10] M. Rosenfeld, D. Kwak, Time-dependent solutions of viscous incompressible flows in moving co-ordinates, *Int. J. Numer. Meth. Fluids* 13 (1991) 1311–1328.
- [11] H.A. Carlson, G. Berkooz, J.L. Lumley, Direct numerical simulation of flow in a channel with complex time-dependent wall geometries: a pseudospectral method, *J. Comput. Phys.* 121 (1995) 155–175.
- [12] S. Xu, D. Rempfer, J. Lumley, Turbulence over a compliant surface: numerical simulation and analysis, *J. Fluid Mech.* 478 (2003) 11–34.
- [13] S. Ogawa, T. Ishiguro, A method for computing flow fields around moving bodies, *J. Comput. Phys.* 69 (1987) 49–68.
- [14] Wei Shyy, H.S. Udaykumar, M.M. Rao, R.W. Smith, *Computational Fluid Dynamics with Moving Boundaries*, Taylor and Francis, Washington, DC, 1996.
- [15] K.S. Sheth, C. Pozrikidis, Effects of inertia on the deformation of liquid drops in simple shear flow, *Comput. Fluids* 24 (2) (1995) 101–119.
- [16] E.A. Fadlun, R. Verzicco, P. Orlandi, J. Mohd-Yusof, Combined immersed-boundary finite-difference methods for three-dimensional complex flow simulations, *J. Comput. Phys.* 161 (2000) 35–60.
- [17] J.G. Oldroyd, On the formulation of rheological equations of state, *Proc. Roy. Soc. A* 200 (1063) (1950) 523–541.
- [18] T. Gal-Chen, R. Somerville, On the use of a coordinate transformation for the solution of the Navier–Stokes equations, *J. Comput. Phys.* 17 (1975) 209–228.
- [19] T. Gal-Chen, R. Somerville, Numerical solution of the Navier–Stokes equations with topography, *J. Comput. Phys.* 17 (1975) 276–310.
- [20] S. Kang, H. Choi, Active wall motions for skin-friction drag reduction, *Phys. Fluids* 12 (12) (2000) 3301–3304.
- [21] K. Akselvoll and P. Moin. Large eddy simulation of turbulent confined coannular jets and turbulent flow over a backward facing step. Technical Report TF-63, Thermosciences Division, Dept. of Mech. Eng., Stanford University, 1995.
- [22] T.R. Bewley, P. Moin, R. Temam, Dns-based predictive control of turbulence: an optimal benchmark for feedback algorithms, *J. Fluid Mech.* 447 (2001) 179–225.
- [23] S. Tsangaris, E. Leiter, On laminar steady flow in sinusoidal channels, *J. Eng. Math.* 18 (1984) 89–103.